The Canadian Mineralogist
Vol. 35, pp. 1379-1390 (1997)

VEIN-TYPE GRAPHITE IN JURASSIC VOLCANIC ROCKS OF THE EXTERNAL ZONE OF THE BETIC CORDILLERA, SOUTHERN SPAIN

JOSE F. BARRENECHEA[1], FRANCISCO JAVIER LUQUE[1] AND MAGDALENA RODAS[1]

Departamento de Cristalografía y Mineralogía, Facultad de Geología, Universidad Complutense de Madrid, E-28040 Madrid, Spain

JILL D. PASTERIS[1]

Department of Earth and Planetary Sciences, Washington University, Campus Box 1169, One Brookings Drive, St. Louis, Missouri 63130-4899, U.S.A.

ABSTRACT

We have investigated volcanic-rock-hosted graphite mineralization in the Huelma area of the Betic Cordillera, in southern Spain, in order to establish the mineralogical characteristics of the graphite and the mechanism of its formation. The graphite is highly crystalline, as revealed by XRD and Raman spectroscopic data, and relatively pure chemically (C content >90 wt.%). XRD data demonstrate that some of the mineralized bodies contain both hexagonal and rhombohedral graphite. Carbon isotopic compositions ($-23.0 < \delta^{13}C < -20.7‰$) and other geological observations indicate that the carbon in the graphite was derived from organic matter included in the metamorphic basement. Cooling of a C–O–H fluid appears to be the most likely mechanism for precipitation of the graphite, although hydration reactions also may have played a role. The presence of rhombohedral graphite is discussed with reference to the kinetics of graphite formation.

Keywords: graphite, fluid deposition, volcanic rocks, X-ray diffraction, Raman spectroscopy, Betic Cordillera, Spain.

SOMMAIRE

Nous avons étudié le graphite des roches volcaniques de la région de Huelma, dans la Cordillère Bétique du sud de l'Espagne, afin d'en établir les caractéristiques minéralogiques et le mécanisme de formation. Il s'agit de graphite à haute perfection cristalline, comme le révèle une étude par diffraction X et par spectroscopie de Raman, et ayant une composition chimique relativement pure (>90% de C, par poids). Selon les données diffractométriques, certains des gisements contiennent à la fois les formes hexagonale et rhomboédrique. Les compositions isotopiques ($-23.0 < \delta^{13}C < -20.7‰$) et autres critères géologiques indiquent que le carbone du graphite serait dérivé de matière organique présente dans le socle métamorphique. Le refroidissement d'une phase fluide contenant C–O–H semble le mécanisme le plus propice à expliquer la précipitation du graphite, quoique des réactions d'hydratation ont aussi pu jouer un rôle. La présence de graphite rhomboédrique s'explique par référence à la cinétique de formation du graphite.

Keywords: graphite, déposition d'une phase fluide, roches volcaniques, diffraction X, spectroscopie de Raman, Cordillère Bétique, Espagne.

INTRODUCTION

Graphite mineralization is commonly associated with metasedimentary rocks, in which it results from the transformation of organic matter by regional or contact metamorphism. Most syngenetic deposits of graphite originate by this process of graphitization (Diessel & Offler 1975, Wada *et al.* 1994). Graphite is also found in many igneous rocks, from felsic to mafic or ultramafic, as vein-like epigenetic deposits (Duke & Rumble 1986, Luque *et al.* 1992, Dissanayake 1994). These authors, among others, have suggested deposition from C-bearing fluids as the mechanism of formation. Carbonic compounds in these fluids may come from the maturation of organic matter, the devolatilization of carbonate-rich materials, and mantle-derived carbon. Until now, the only known minable concentration of graphite associated with volcanic rocks occurs at Borrowdale, England, where the graphite replaces primary minerals within a series of hydrothermally altered andesites of Ordovician age, forming irregular to nodular concentrations (Strens 1965, Weis *et al.* 1981).

[1] *E-mail addresses*: barrene@eucmax.sim.ucm.es, jluque@eucmax.sim.ucm.es, rodas@eucmax.sim.ucm.es, pasteris@levee.wustl.edu

In this work, we describe an example of volcanic-rock-hosted graphite in vein-type occurrences located in the external zone of the Betic Cordillera, in southeastern Spain. We document the mineralogical, crystallochemical, and isotopic characteristics of this graphite in order to elucidate the possible source of the carbon, and the mechanism of formation of the graphite in relation to the evolution of the volcanic host-rocks.

Geological Setting

The study area is located within the Subbetic Domain of the External Zone of the Betic Cordillera, which represents the westernmost range of the Mediterranean Alpine Belt (Fig. 1). During the Mesozoic, the External Zone of the Betic Cordillera formed a passive continental margin in southern Iberia (García-Hernández *et al.* 1980), from Middle to Late Jurassic time (155–166 ± 4 Ma; Portugal *et al.* 1995). Submarine volcanic activity occurred in relation to a complex system of fractures having a regional NE–SW trend (Comas *et al.* 1986). Magmatism in this area has been linked to a transtensional regime associated with the opening of the Atlantic Ocean (García Dueñas & Comas 1983).

The volcanic rocks occur in discontinuous outcrops along a NE–SW belt about 250 km long and 5–10 km wide (Fig. 1). Principal rock-types are pillow lava and pillow-breccia flows, with local intercalations of hyaloclastite (Puga *et al.* 1989). The flows range in total thickness from several dozens of meters to about 1 km (Puga & Portugal 1989), with individual outcrops comprising a few square kilometers. Sills and dykes also are common. Major differences in bulk chemical composition, mineral assemblage, and mineral composition are related to complex processes of differentiation (see below). All of the igneous rocks are interbedded with a sequence of pelagic carbonate sedimentary rocks, dominantly marl and limestone.

On the basis of distribution patterns of major and incompatible trace-elements, three units (lower, middle, and upper) can be distinguished within the volcanic pile; these show an increasing degree of contamination with crustal material from bottom to top (Puga & Portugal 1989). These members are correlated with the interlayered sedimentary facies. In particular, crustal contamination of the igneous rocks of the upper unit originated in conjunction with a period of tectonic activity in the basement that affected the walls of fairly shallow magma-chambers, triggering the assimilation of metapelitic rocks.

According to Puga *et al.* (1989), rocks of the lower unit are poorly differentiated alkali olivine basalts. At some sites, the middle and upper units contain xenoliths of pelitic rocks (with partially replaced crystals of andalusite, chloritoid, and staurolite), which are interpreted as fragments from a subcropping metamorphic basement. Puga & Portugal (1989) concluded that the rocks of the middle and upper units represent basalts differentiated by the following processes: fractional crystallization, assimilation of pelitic rocks, and incorporation of a K-rich fluid phase (which accounts for the anomalously high contents of K found in most rocks of the upper unit). These authors further suggested that recrystallization and partial melting of the pelitic fragments occurred in two stages (silicate and oxide), with temperatures reaching 600°C and 1360°C, respectively, whereas the pressure remained less than 1 kilobar.

Analytical Methods

The structural features and chemical composition of graphite and its thermal behavior were studied in concentrates obtained by acid treatment as described by Luque *et al.* (1993). Structural parameters, including interplanar spacings (d_{002}), crystallite size along the *c* axis (*Lc*), and the degree of graphitization (u), were determined by X-ray diffraction (XRD) on bulk concentrates of graphite. Diffraction analyses were carried out with a Philips PW 1729 X-ray diffractometer using Cu$K\alpha$ radiation at 40 kV and 30 mA, a graphite monochromator, a step size of 0.01 (°2θ), time per step of 0.5 s, scan speed of 0.02 (°2θ/s), and receiving slit of 0.1 mm. Samples were run from 20 to 65°2θ. Silicon was used as an internal standard.

Physical characteristics on the scale of individual grains were obtained by means of Raman microprobe spectroscopy. This technique provides information on the crystallite size within the (001) basal plane of the graphite (that is, the crystallite size along the *a* axis, *La*); the degree of crystallinity increases as *La* increases. The characteristics of the Raman spectra as a function of graphite crystallinity were discussed and illustrated in Pasteris & Wopenka (1991), Wopenka & Pasteris (1993), and references therein. Raman spectroscopy was performed on grain separates, on unpolished, carefully broken fragments of veins of millimeter-scale thickness, and on small nodule-like concentrations, in order to test for variations in crystallinity from the inner to the outer parts of the graphite occurrences (see below). Raman microprobe analyses were acquired using a Jobin–Yvon triple-monochromator S3000 laser Raman microprobe. All three stages of the monochromator have holographic gratings with 600 grooves/mm. The sample was excited by an argon-ion laser using the 514.5 nm green line, with about 10mW power at the sample surface. The same Olympus MS Plan 80× ultralong-working-distance microscope objective (N.A. = 0.75) was used to image the sample optically, focus the laser beam to approximately 1 μm in diameter, and capture the Raman-scattered radiation for detection by a 1024-channel intensified optical diode array detector (2.54 cm, proximity-focused). Operated in this mode, the system has a spectral resolution of about 7 cm^{-1}.

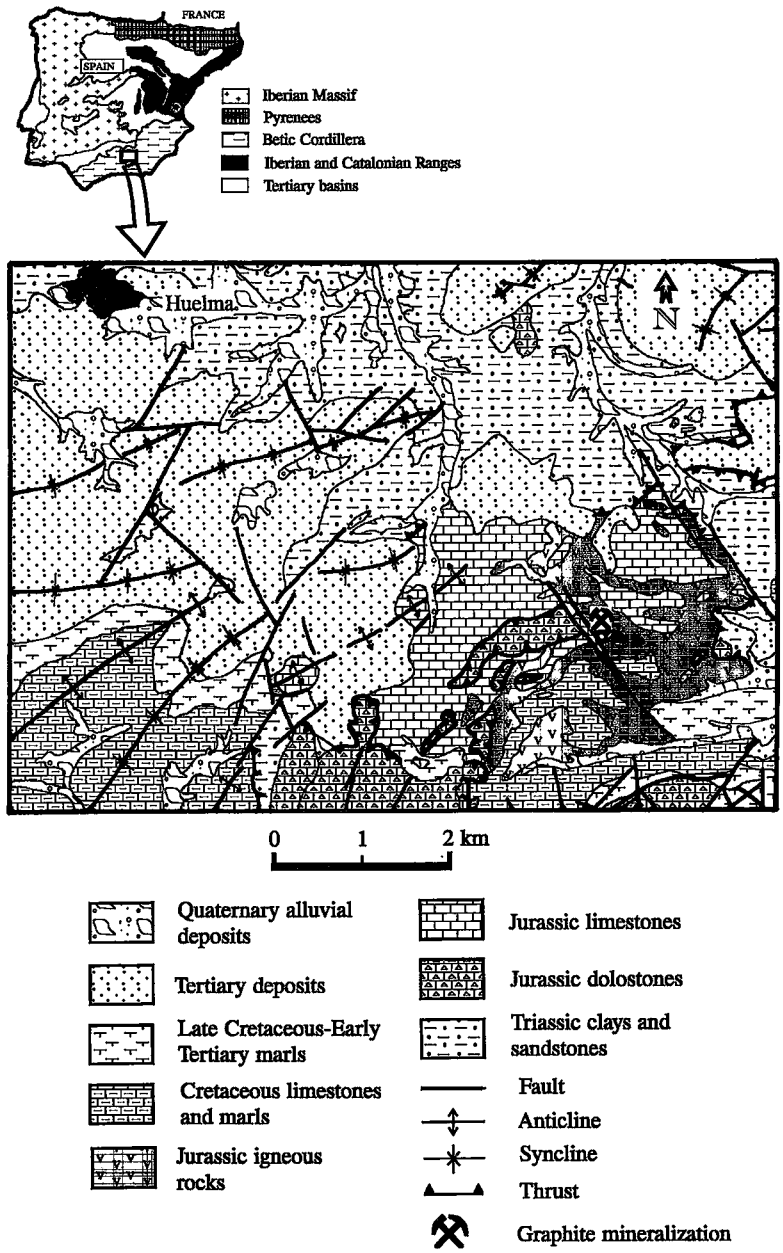

FIG. 1. Geological setting of the study area. Modified after Díaz de Neira *et al.* (1991).

The thermal properties of graphite were determined by simultaneous recording of differential thermal analysis (DTA) and thermogravimetric (TG) curves, using a Stanton STA 781 apparatus. The DTA curves of graphite were obtained by heating the sample at 10°C/min in the range 20°C to 1000°C, with a continuous air supply of 50 mL/min. Under these analytical conditions, the exothermic maximum due to carbon combustion can be interpreted in terms of graphite crystallinity: DTA maxima shift to higher temperatures as crystallinity increases (Kwiecinska 1980, Wada *et al.* 1994). The DTA maximum is accompanied by a weight loss (as recorded in the TG curve) whose magnitude depends on the carbon content of the graphite sample. Estimated contents of carbon based on the TG curves were verified by elemental analysis of the samples using a Perkin–Elmer CHN 2400 gas analyzer for the determination of C, H, and N concentrations. The analyses were done at 925°C, with acetanilide used as a standard.

Geochemical characterization of the graphite also included determination of the ratio of the stable carbon isotopes on selected samples; the analyses were performed at Geochron Laboratories (Cambridge, Massachusetts). Samples selected for isotopic analysis include 1) bulk concentrates of graphite obtained by acid treatment, and 2) powdered samples obtained from small holes (1 to 2 cm apart) excavated using a steel needle on unweathered surfaces of some of the largest veins and nodules; although these powders contain silicate impurities, their graphite contents allowed for reproducible analyses. Graphite samples were burned in pure oxygen in the presence of CuO at 850°C to produce CO_2 for analysis. The CO_2 gas was purified cryogenically by passing it through a dry ice – alcohol trap to remove H_2O, and then trapped in two liquid nitrogen traps. The trapped CO_2 was transferred to a sample flask, and the $^{13}C/^{12}C$ of the CO_2 was determined on a VG Micromass gas-source mass spectrometer (model 903). Results are given in the standard $\delta^{13}C$ notation relative to the PDB standard. The overall precision of the method, including preparation and analysis, is about ±0.2‰.

Chemical compositions of primary minerals in the volcanic host-rocks were obtained by electron-microprobe analysis with a JEOL Superprobe JXA 8900–M, under the following instrumental conditions: accelerating voltage 15 kV, current 20 nA, and beam diameter 5 μm. Standards of similar compositions to the analyzed minerals were used [see Jarosewich *et al.* (1980) for details on the standard samples].

Graphite Mineralization

The mineralization studied (Fig. 1) is associated with one volcanic outcrop of the upper unit located southeast of Huelma, in Jaén Province. The host rock is a basaltic sill, overlain by a thick layer of pillow-lava flows in which carbonate forms the inter-pillow material. Graphite is very localized, occurring exclusively within the sill. No other deposits of graphite have been found in the area. The sill has the composition of an alkali basalt, and an intergranular to intersertal texture. Phenocrysts include titaniferous augite, olivine, plagioclase, and alkali feldspar, with corundum, spinel, and rutile as the main accessory phases. Representative compositions of these minerals are listed in Table 1. The groundmass is made up of plagioclase and minor augite and Fe–Ti oxides.

TABLE 1. CHEMICAL COMPOSITION* OF PRIMARY MINERALS IN THE IGNEOUS HOST-ROCK AND OF SPINEL DERIVED FROM THE ASSIMILATION OF METAPELITIC BASEMENT

	Cpx (14)		Pl (19)		Nafs (9)		Kfs (6)		Spl (7)	
	$\bar{x}$	σ	$\bar{x}$	σ	$\bar{x}$	σ	$\bar{x}$	σ	$\bar{x}$	σ
SiO_2	49.21	1.64	52.44	1.79	66.60	0.83	64.67	0.46	0.00	
Al_2O_3	3.12	0.75	29.90	1.64	20.56	0.51	18.67	0.12	65.64	0.31
FeO¶	9.16	2.62	0.24	0.08	0.13	0.06	0.09	0.01	17.58	0.22
MnO	0.19	0.06	0.00		0.00		0.00		0.18	0.04
MgO	15.13	2.74	0.12	0.03	0.00		0.01	0.00	16.23	0.16
CaO	21.10	1.05	12.49	1.54	0.29	0.13	0.01	0.00	0.00	
Na_2O	0.34	0.14	4.39	0.82	11.30	1.05	0.31	0.10	0.00	
K_2O	0.00		0.21	0.08	0.67	0.13	16.54	0.51	0.00	
TiO_2	1.52	0.63	0.07	0.03	0.00		0.01	0.00	0.20	0.05
NiO	0.01	0.02	0.01	0.01	0.00		0.00		0.06	0.01
Cr_2O_3	0.38	0.32	0.00		0.00		0.00		0.03	0.01
Total	100.16		99.87		99.55		100.31		99.92	

* The proportion of major-element oxides is reported in wt.%. ¶ Total Fe is reported as FeO. Average values, expressed by $\bar{x}$, are derived from results of the number of analyses shown in parentheses. The standard deviation is given by σ. Symbols: Cpx clinopyroxene, Pl plagioclase, Nafs sodium-dominant alkali feldspar, Kfs potassium-dominant alkali feldspar, Spl spinel.

The most abundant ferromagnesian phenocryst is titaniferous augite, which forms subhedral to anhedral crystals ranging from 0.5 to 1.5 mm across; they have a uniform composition. Olivine, a less abundant phenocryst, is mostly replaced by smectite-group minerals and chlorite-group minerals; its composition ranges from Fo_{78} to Fo_{65} (Comas *et al.* 1986, Puga *et al.* 1989). Plagioclase forms euhedral phenocrysts 0.1 to 0.8 mm long, and is locally replaced by calcite. Within a single thin section, plagioclase may range in composition from labradorite to albite. The grains of alkali feldspar are compositionally zoned from Na- to K-rich members (Table 1). Spinel occurs as aggregates of small (up to 0.1 mm) purple grains; we believe that it formed by reaction of basaltic magma with aluminosilicate minerals (Puga & Portugal 1989). Rutile forms isolated acicular crystals or dendritic aggregates, varying in size from fine-grained in the mesostasis to 0.5-mm-long phenocrysts. Secondary minerals in the basalts include chlorite- and smectite-group minerals that mainly formed after olivine, and calcite that fills small voids and cracks, both in the phenocrysts and the mesostasis.

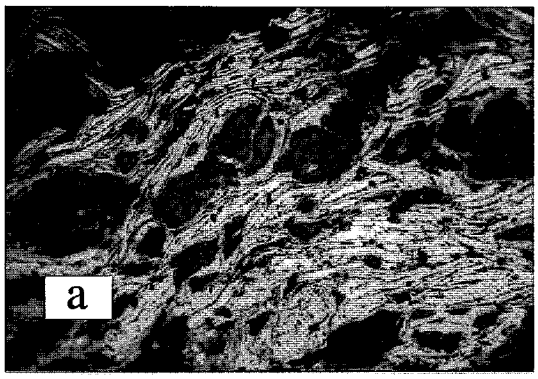

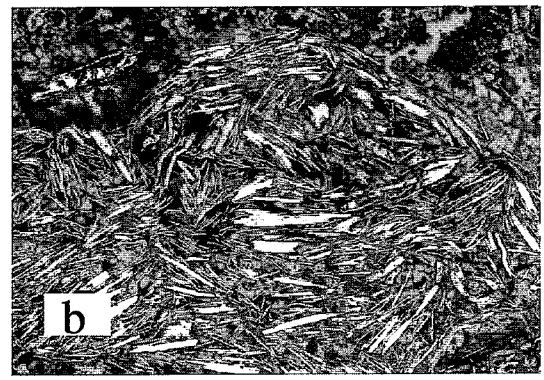

FIG. 2. Reflected-light photomicrographs showing textural characteristics of the graphite. a) Flakes of graphite (light grey) surrounding breccia fragments of the host rock (dark grey). Note that the flakes parallel the contacts. b) Aggregate of randomly oriented flakes of graphite (light grey) forming a nodule-like concentration. The width of the field of view in both cases is 2.5 mm. c) Natural surfaces of carefully broken vein of graphite. Differences in brightness within a light region indicate deviations from horizontality of the crystal faces. Largest dimension of photo is 125 μm.

Graphite mineralization occurs dominantly as fracture-filling veins, although small nodules and rounded to irregular pocket-like bodies of graphite have been observed where two or more of the veins cut each other. The veins vary in thickness from a few millimeters up to 20 cm, with graphite as the only mineral in them. Nodules are typically 0.5 to 3 cm in diameter, whereas pocket-like bodies are up to 20–25 cm along the greatest dimension. Some areas within the graphite veins show signs of brecciation, with graphite being distributed around breccia fragments. In general, the contact between the graphite and the host rock is sharp, although in some cases it is gradational. Calcite and quartz veinlets ranging in thickness from a few millimeters to several centimeters occur in association with the graphite mineralization. No signs of graphite were found in the surrounding carbonate sediments or in the pillow lavas.

In polished slabs, the graphite forms flakes ranging in size from 50 to 800 μm, and is more strongly reflectant than kerogen, coalified organic matter, and poorly crystalline graphite. Within the veins, the flakes are oriented predominantly parallel to the vein walls; graphite crystals typically occur as coatings around breccia fragments (Fig. 2a). Within the nodules, graphite flakes are randomly distributed, and lack a preferred orientation (Figs. 2b, c). Graphite has not been found disseminated in the host rock; together with the presence of the veins, this finding suggests an epigenetic character for the mineralization.

The structural parameters of these samples of graphite obtained by XRD, namely c_o, the stacking height along the [001] direction (Lc), and the degree of graphitization (u), are summarized in Table 2. Generally speaking, the narrower and more symmetrical the (002) peak, the greater the Lc and u values. In addition, d_{002} values increase from well-ordered (d_{002} = 3.35 Å) to disordered graphite (d_{002} > 3.35 Å). Values of these parameters indicate a perfect three-dimensional order for the graphite studied here. The non-basal reflections of hexagonal graphite are also recorded in the XRD patterns (Fig. 3). In addition, the ratio of height to width of the (002) reflection, the intensity ratio of the (002) and (004) diffraction peaks, and the symmetry of the (002) reflection, deduced from the values of d_{002} at half height and at one-third of the peak height, are also within the range expected for fully ordered graphite (Landis 1971).

TABLE 2. X-RAY-DIFFRACTION PARAMETERS OF GRAPHITE FROM THE JURASSIC VOLCANIC HOST-ROCKS, COMPARED TO THOSE OF FULLY ORDERED GRAPHITE

	Betic Cordillera	Fully ordered
$d_{(002)}$ (Å) (at I_{max})	3.351 – 3.356	3.35 – 3.36
c_0 (Å)	6.702 – 6.712	6.70 – 6.72
$d_{(002)}$ (Å) (½W at ½H)	3.351 – 3.358	3.35 – 3.36
$d_{(002)}$ (Å) (½W at ⅛H)	3.351 – 3.358	3.35 – 3.36
$d_{(002)}$ H/W (at ½H)	45 – 75	30
$I_{(002)}/I_{(004)}$	15 – 25	–
D.G. (u)	>0.85	–
Lc (Å)	>650	
Proportion (%) of rhombohedral polytype	0 – 25	
No. samples	23	

The parameters of fully ordered graphite are taken from Landis (1971). H: peak height, W: peak width, D.G. (u): degree of graphitization, given by $[d_{002} = 3.440 - 0.086\ (1 - p^2)]$, where $p = (1 - u)$ (Kwiecinska 1980).

Literature reports indicate that in most natural occurrences, graphite is hexagonal, and that where the rhombohedral phase is present, it seems to decrease in abundance as temperature of formation increases. The two polytypes of graphite (hexagonal and rhombohedral) can be distinguished by XRD analysis, since the diffraction pattern of each type shows some diagnostic reflections. Relative amounts of each phase can be evaluated by means of the intensity ratio of specific peaks (Kwiecinska 1980). The XRD patterns of some of the graphite samples studied here show two peaks, at 2.08 Å and 1.97 Å, which correspond to the (101) and (012) reflections, respectively, of the rhombohedral polytype (Fig. 3). On the basis of the intensity ratio of the (101) diffraction peaks for both hexagonal and rhombohedral graphite, the content of the rhombohedral phase within these samples is estimated to be up to 25%. The partially overlapping (101) peaks for both hexagonal and rhombohedral graphite were deconvolved using the Philips PC–APD (version 3.6) software, which is based on the mathematical model described by Schreiner & Jenkins (1983).

At the XRD scale, graphite appears to have a fairly homogeneous degree of order from one mineralized body to another. Moreover, within any individual vein or pocket-like body, no significant variations in crystallinity or content of rhombohedral phase has been found in the XRD patterns of samples taken from the inner to the outer parts of these occurrences. The main difference among mineralized bodies lies in the abundance of the rhombohedral phase, which may be absent in some areas.

Determination of structural features by Raman microprobe spectroscopy was carried out on both grain separates and freshly broken, unpolished fragments. A total of 82 grains from three different mineralized bodies were analyzed, and ratios of the "disorder peak" (*D*) to the "order peak" (*O*) in the spectra were calculated. About 70% of the spectra correspond to perfectly

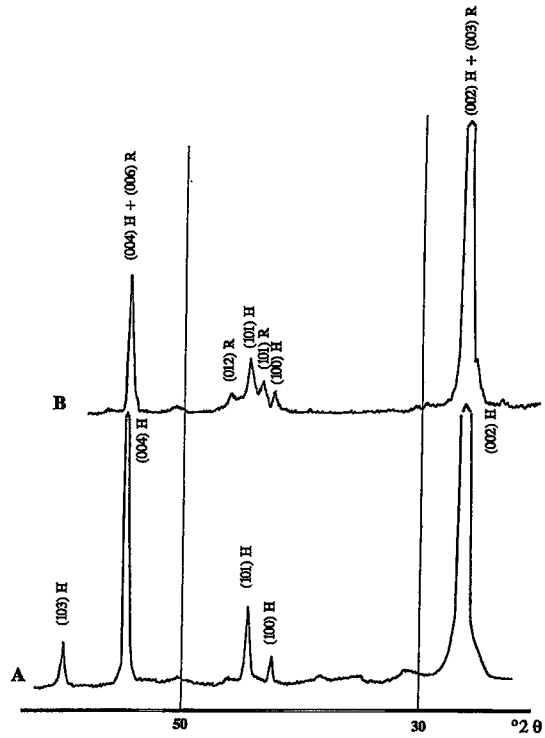

FIG. 3. XRD patterns of both hexagonal (H) and hexagonal + rhombohedral (R) graphite in samples from two mineralized vein-like bodies. The spacing and symmetry of the (002) and (002 + 003) peaks indicate a high degree of order.

ordered graphite (*D*:*O* = 0; Fig. 4). However, slightly disordered graphite also was found, having a mean *D*:*O* ratio of 0.07 (one grain shows a *D*:*O* ratio of 0.16). The overall spectral characteristics of these samples of graphite reveal a high degree of order along the *a* axis. According to the estimation of Wopenka & Pasteris (1993), the size of such in-plane crystallites along the [100] direction (*La*) is larger than 2000 Å, and corresponds to that of graphite crystallites in carbonaceous metapelites in the granulite facies.

In addition, Raman spectra of individual flakes analyzed *in situ* in samples from the inner to the outer parts of veins and "nodules" (Fig. 2c) indicate the same degree of order and homogeneity as the analyses reported above on grain separates.

The DTA curve shows a strong exothermic peak in the range 660–730°C due to graphite combustion (Fig. 5). Such temperatures for the DTA maximum suggest a high degree of order, comparable to that observed in graphite from amphibolite-facies terranes (Kwiecinska 1980). Carbon contents calculated from the weight loss on the TG curves are greater than 90 wt.%, in good

agreement with the results obtained by elemental analysis.

The carbon isotope signature of the graphite samples is quite homogeneous and falls in a narrow range of $\delta^{13}C$ values from –23.0 to –20.7‰. Samples collected at different distances from the contact between mineralized bodies and host rocks on a scale of 1–2 cm apart lack isotopic zoning, and show very constant $\delta^{13}C$ values within single veins or pocket-like bodies. Even in the relatively large mineralized bodies that are cut by calcite veinlets, no significant isotopic variations are observed in the vicinity of the carbonates (Fig. 6).

Origin of the Graphite

Any discussion on the formation of fluid-deposited graphite must deal with aspects of the source of the carbon and mechanisms of its mobilization and precipitation. In this section, we discuss these issues with reference to the system C–O–H, in which most igneous and metamorphic fluids reasonably can be represented. Relationships in this system provide a good model for the deposition of graphite from fluids.

The most reliable information on the provenance of carbon contained in the graphite is provided by the carbon isotopic ratio ($^{13}C/^{12}C$) of the graphite itself, although other geological and mineralogical evidence must be taken into account. There are three main potential sources of carbon in fluids: a) Carbon-bearing gases may be released during maturation of organic matter. Such biogenically derived, reduced carbon is enriched in ^{12}C, with $\delta^{13}C$ values in the range –40 to –15‰ (Hahn-Weinheimer & Hirner 1981, Schidlowski *et al.* 1983, Crawford & Valley 1990). b) Carbon may be produced by the devolatilization of carbonate minerals. Such oxidized carbon is enriched in ^{13}C. Once incorporated into a fluid, this type of carbon should lead to the formation of an isotopically heavier graphite than that in a), *i.e.*, $\delta^{13}C$ –5 to +5‰ (Hahn-Weinheimer & Hirner 1981, Weis *et al.* 1981). c) The carbon may be mantle-derived. Graphite precipitated from such carbon-bearing fluids show intermediate isotopic ratios, with $\delta^{13}C$ values ranging between about –9.8 and –4.8‰ (Pearson *et al.* 1990).

The interpretation of isotopic data, however, usually is complicated by the influence of other processes that may modify the original isotopic signature.

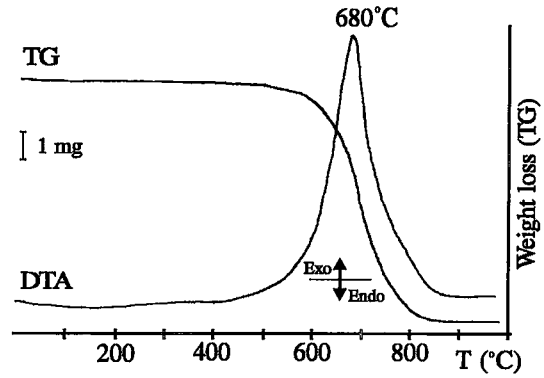

FIG. 5. Differential thermal analysis (DTA) and thermogravimetry (TG) curves for graphite, showing the exothermic effect and the weight loss due to the combustion of carbon. Initial weight: 9.45 mg. Heating rate: 10°C/min.

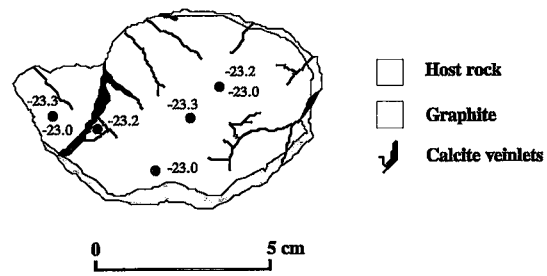

FIG. 6. Sketch of a hand sample of a graphite nodule showing $\delta^{13}C$ values (in ‰). Dots represent sample locations for different parts of the nodule. Host rock corresponds compositionally to an alkali basalt.

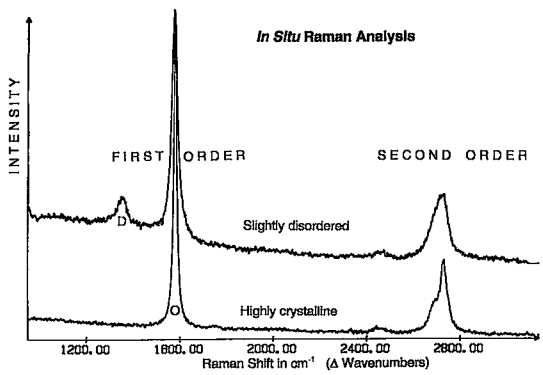

FIG. 4. Raman spectra of grains of graphite from Huelma analyzed *in situ* in broken nodules of graphite. Bottom spectrum is representative of the highly ordered graphite that is characteristic of these deposits; the upper spectrum represents slightly disordered graphite that is much less abundant. Both first-order and second-order spectral features shown. As intensity of disorder-induced peak (D) increases in the first-order spectrum, the size of the crystallites measured along the basal plane decreases.

Changes in the temperature of the fluid during the deposition of graphite (Bottinga 1969), mixing of fluids from different provenances (Rumble & Hoering 1986), and changes in the ratio CO_2/CH_4 of the fluid (Duke & Rumble 1986) affect the magnitude of the isotopic fractionation. Thus, the isotopic signature of fluid-deposited graphite records both the source of carbon and modifications of the fluids during different stages of graphite precipitation.

Graphite mineralization of the Betic Cordillera has a fairly uniform $\delta^{13}C$ signature (–23.0 to –20.7‰) that suggests an organic origin for the carbon species contained in the graphite-depositing fluids. It is likely that the carbon was derived from the devolatilization of organic matter within the non-outcropping metamorphic basement, which was partially assimilated by the igneous rocks. The presence of carbonaceous matter in these metamorphic rocks is shown by opaque inclusions in the andalusite xenocrysts ("chiastolite") in volcanic rocks of the upper unit. Values of $\delta^{13}C$ for such carbonaceous inclusions are not available. In addition, the small isotopic differences observed among graphite samples taken from various bodies suggest that deposition occurred over a narrow range of temperature and from fluids that had essentially a uniform composition. For each mineralized body, the lack of isotopic zoning and the textural homogeneity point to a process of precipitation developed during a single stage. Furthermore, the observed homogeneity of the graphite isotopic signature in proximity to calcite veinlets indicates that the carbonate-precipitating fluids or the conditions under which they precipitated were unsuitable for the formation of graphite. Indeed, these homogeneous $\delta^{13}C$ values suggest a lack of reaction between the previously formed graphite and later carbonate-bearing fluids. This observation indicates that isotopic exchange did not proceed once graphite was fully crystallized, probably because of the very sluggish kinetics of diffusion of carbon in graphite (Chacko *et al.* 1991, Dunn & Valley 1992, Scheele & Hoefs 1992).

Additional evidence exists for fluid–rock–melt interaction in this rock suite. Petrographic studies of the volcanic host-rock reveal a hydrothermal–metasomatic stage, in which potassium-rich feldspar overgrew plagioclase crystals, and a volatile-rich fluid phase (with H_2O and some CO_2) promoted replacement of some mafic phases (mainly olivine and pyroxene) by chlorite, a smectite-group mineral, iron oxides, and carbonates (Puga & Portugal 1989). The effects of this late metasomatism are widespread over most of the rocks of the upper unit, and it has affected the host rocks intensely. This overprint would explain why graphite veining is restricted to this outcrop. Puga & Portugal (1989) further suggested that the potassium-rich fluid resulted from dehydration and breakdown of the major phases of the metamorphic xenoliths (especially muscovite and biotite) that took place during recrystallization of the pelitic rocks. This fluid may have been enriched in carbon-bearing species as a consequence of the decomposition of carbonaceous matter dispersed in the assimilated metamorphic rocks. Such thermal breakdown would be an ongoing process, and would maintain carbon enrichment in the magma chamber throughout the period of contamination. Unfortunately, the metamorphic basement does not crop out, and there is only indirect evidence on the nature of the organic matter content of these rocks, as inferred from the "chiastolite"-bearing xenoliths.

As shown in the experimental work of Ziegenbein & Johannes (1980), in a C–O–H system, carbon will be incorporated in the fluid phase as H_2O-soluble mobile gases (mainly CH_4 and CO_2). The transfer of carbon from this homogeneous C–O–H fluid into an aqueous fluid that coexists with graphite takes place through molecular reactions of the type $CO_2 + CH_4 = 2C + 2H_2O$. Such reactions depict the transport of carbon *via* gaseous species and its eventual precipitation as graphite (Walther & Althaus 1993).

The size of the stability field of graphite is sensitive to geologically controlled intensive parameters. The graphite + fluid stability field becomes larger as temperature decreases at constant pressure, or as pressure increases at a fixed temperature (Fig. 7). Both of these processes favor the deposition of graphite, as the graphite field overtakes and incorporates a specific C–O–H bulk composition of interest (Ohmoto & Kerrick 1977, Ziegenbein *et al.* 1989). Isobaric cooling probably is the most effective way to promote precipitation of graphite from a fluid in any geological context, and especially in the veins studied here. In addition to these isochemical changes that cause the deposition of graphite from fluids, there are (isobaric–isothermal) changes in fluid chemistry that can induce its precipitation. For example, hydration reactions can deplete a fluid in H_2O, thereby enriching it in carbon and promoting graphite precipitation (Rumble *et al.* 1986).

Reference to Figure 7 and the above discussion indicates the difficulty in determining the specific P–T–*X* conditions under which graphite was deposited. However, additional information is available from the crystallographic form and degree of crystallinity of the precipitate. Most natural examples of graphite, originating both from the metamorphism of carbonaceous matter and from deposition by fluids, are of the hexagonal form. The percentage of the rhombohedral phase in "metamorphic" graphite decreases with increasing grade of metamorphism. The rhombohedral polytype in such graphite is considered to have formed during growth of the hexagonal structure (Kwiecinska 1980). In contrast with the wide-ranging crystallinity of metamorphic graphite, fluid-deposited graphite commonly displays a uniform crystallinity in occurrences worldwide. This observation stands in contrast to experimental results, showing that

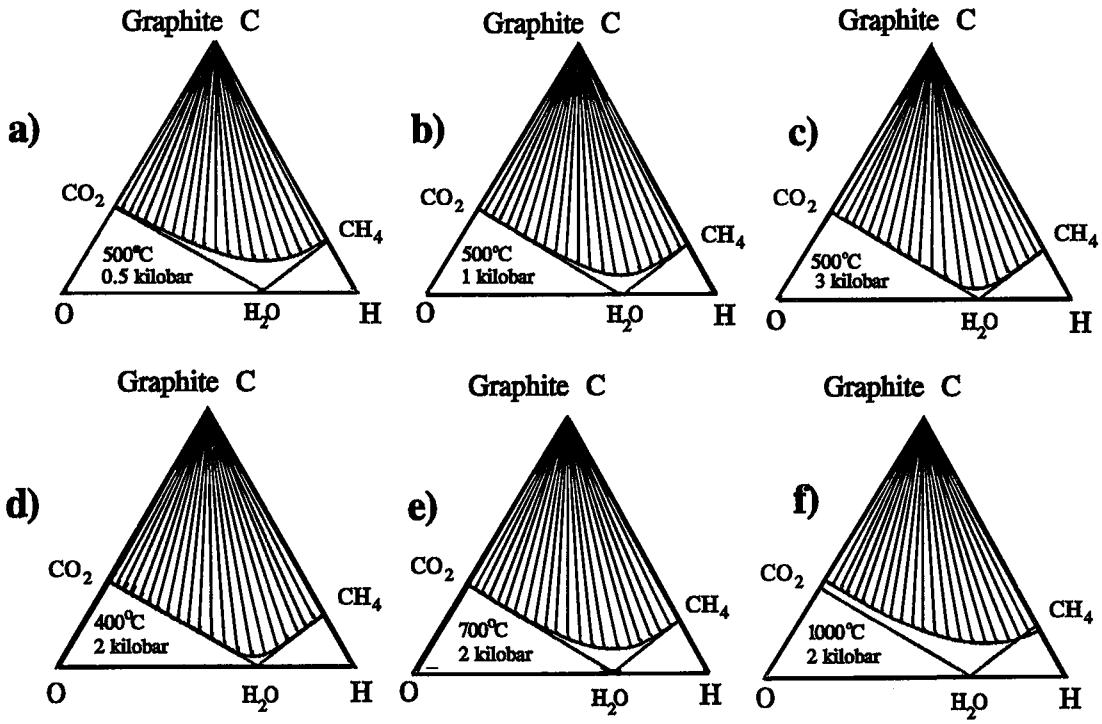

FIG. 7. Isothermal, isobaric sections for the system C–O–H showing the two-phase field (tie lines shown) where graphite coexists with fluid. Sections a, b, and c show the effect of increasing pressure at fixed T. Sections d, e, and f show the effect of increasing temperature at fixed P. Modified from Ferry & Baumgartner (1987, p. 359), reprinted with the permission of the Mineralogical Society of America.

poorly ordered graphite may precipitate from C–O–H fluids (Ziegenbein & Johannes 1990, Krautheim 1993, Pasteris *et al.* 1995, Pasteris & Chou 1998). Not only does the crystallinity of fluid-deposited graphite reflect its temperature of deposition, but the thermochemical properties of "disordered" graphite also differ from those of well-crystalline graphite. This distinction leads to a smaller field of stability for poorly crystalline graphite (Fig. 8; Ziegenbein & Johannes 1990).

Graphite from vein mineralization of the Betic Cordillera therefore stands out because it is both highly crystalline (suggesting high temperature) and contains significant proportions of the rhombohedral polytype (suggesting lower temperature). These characteristics also have been found in the volcanic-rock-hosted graphite deposit at Borrowdale, where up to 31.9% of the rhombohedral polytype has been reported in graphite samples (Kwiecinska 1980). Such features may be related to the specific process of graphite formation. Since deposition of a solid phase from a fluid involves both nucleation and grain growth, kinetic factors may affect the precipitation and physical properties of the graphite. Ziegenbein & Johannes (1980) have shown that graphite–fluid equilibration can be very sluggish at temperatures below 700°C. Thus, at low temperatures, it may be easier to nucleate poorly ordered graphite than well-crystallized graphite. Recent experimental work by Pasteris & Chou (1998) suggests that the graphite initially precipitated from C–O–H fluids is very poorly ordered, and that its degree of crystallinity increases to some maximum with increasing duration of the experiment. For natural fluid-deposited graphite, it is possible that above some undetermined temperature, the larger size of the stability field of fully ordered graphite than that of disordered graphite would be the main controlling factor in this precipitation process, which would favor the crystallization of well-ordered graphite.

The relative abundance of the rhombohedral polytype of graphite in the Betic Cordillera occurrences (and also in the volcanic-rock-hosted deposit at Borrowdale) therefore may represent an intermediate, metastable case between poorly ordered graphite and the more common fully ordered hexagonal phase. If true, then occurrence of the rhombohedral polytype has the same significance in the evolution of the graphitization process for fluid-deposited graphite as for metamorphic graphite. Preservation of the

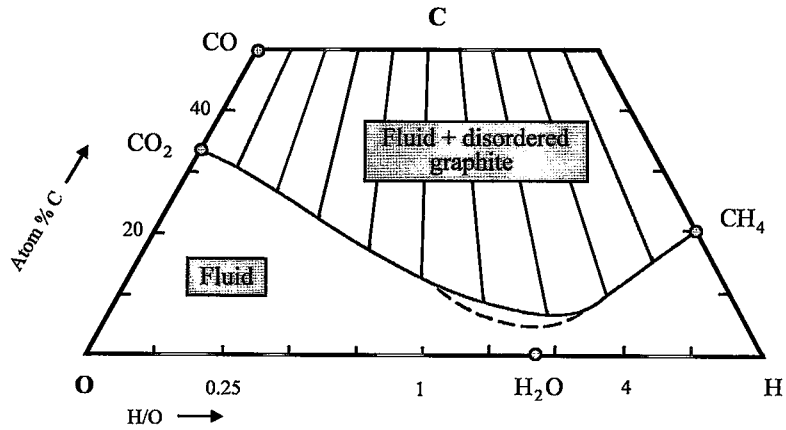

FIG. 8. Representation of the system C–O–H at fixed P–T conditions (400°C and 2 kilobars). The minimum C-content of a fluid in equilibrium with disordered graphite (solid curve) and with fully ordered graphite (dashed curve) is taken from Ziegenbein & Johannes (1990, p. 559), and is reprinted with the permission of the authors.

rhombohedral graphite within mineralization of the Betic Cordillera and at Borrowdale may be induced by a high rate of cooling, as inferred for volcanic environments.

Fluid deposition of graphite in the Betic Cordillera also could have been achieved through hydration reactions. The replacement of primary mafic minerals of the igneous host-rock (mainly olivine and pyroxene) by hydrous phases like chlorite indicates that hydration reactions occurred in the volcanic rocks through hydrothermal activity. Such reactions would remove H_2O from the fluid, which would cause the latter to become enriched in carbon, thus favoring graphite precipitation (Rumble *et al.* 1986, Ziegenbein & Johannes 1990).

In conclusion, the graphite mineralization studied in this paper is believed to have formed as a carbon-bearing fluid passed through the subvolcanic host-rocks. Carbon in the fluid was derived from devolatilization reactions occurring in the assimilated metamorphic rocks. Graphite precipitated as the fluids cooled and underwent H_2O-consuming reactions that caused the formation of a secondary, hydrated mineral assemblage. The presence of both hexagonal and rhombohedral graphite was controlled by the kinetics of precipitation.

The distribution of the graphite (predominantly in veins) may reflect circulation of fluids through tectonically weakened or altered zones. Hydraulic fracturing can be promoted by fluid pressure in such zones, leading to the formation of epigenetic veins of graphite, as indicated by fragments of volcanic rocks (hydraulic brecciation; Jébrak 1992) within the mineralized bodies. Therefore, the concentration of graphite in the veins is readily attributable to the ability of fluids to pass through and even enlarge open fractures. The occurrence of graphite veins in subvolcanic rock-types (*i.e.*, sills) would be more likely, since submarine volcanic rocks (*i.e.*, pillow-lava flows) are dramatically outgassed during eruption, as seen at recent spreading centers on the sea floor.

ACKNOWLEDGEMENTS

The authors are indebted to R. Rojas and J. Parras for assistance during the thermal study and elemental analysis of graphite, respectively, and to B. Wopenka for assistance with Raman analyses. Technicians of the Centro de Microscopía Electrónica de la U.C.M. are also acknowledged for assistance during electron-microprobe analysis. Thanks are also due to M.L. Otter (Geochron Laboratories), who provided information on the analytical equipment and conditions for carbon isotopic analysis. We are indebted to S. Castaño for help with line drawings. The final version of this paper has been improved by reviews from I-Ming Chou and J. Farquhar. This study was supported by the Spanish DGICYT through project PB93–0064, and by the U.S. National Science Foundation through grant EAR91–16967 to JDP.

REFERENCES

BOTTINGA, Y. (1969): Calculated fractionation factors for carbon and hydrogen isotope exchange in the system calcite – carbon dioxide – graphite – methane – hydrogen – water vapor. *Geochim. Cosmochim. Acta* **33**, 49-64.

CHACKO, T., MAYEDA, T.K., CLAYTON, R.N. & GOLDSMITH, J.R. (1991): Oxygen and carbon isotope fractionation between CO_2 and calcite. *Geochim. Cosmochim. Acta* **55**, 2867-2882.

COMAS, M.C., PUGA, E., BARGOSSI, G.M., MORTEN, L. & ROSSI, P.L. (1986): Paleogeography, sedimentation and volcanism of the central Subbetic Zone, Betic Cordilleras, southern Spain. *Neues Jahrb. Geol. Paläont., Monatsh.*, 385-404.

CRAWFORD, W.A. & VALLEY, J.W. (1990): Origin of graphite in the Pickering gneiss and the Franklin marble, Honey Brook Upland, Pennsylvania Piedmont. *Geol. Soc. Am., Bull.* **102**, 807-811.

DÍAZ DE NEIRA, J.A., ENRILE, A. & LÓPEZ OLMEDO, F. (1991): Hoja n. 970 (Huelma) a escala 1:50.000 del Mapa Geológico de Nacional (MAGNA). Instituto Tecnológico Geominero de España, Madrid, Spain.

DIESSEL, C.F.K. & OFFLER, R. (1975): Change in physical properties of coalified and graphitised phytoclasts with grade of metamorphism. *Neues Jahrb. Mineral., Monatsh.*, 11-26.

DISSANAYAKE, C.B. (1994): Origin of vein graphite in high-grade metamorphic terrains. Role of organic matter and sediment subduction. *Mineral. Deposita* **29**, 57-67.

DUKE, E.F. & RUMBLE, D., III (1986): Textural and isotopic variations in graphite from plutonic rocks, south central New Hampshire. *Contrib. Mineral. Petrol.* **93**, 409-419.

DUNN, S.R. & VALLEY, J.W. (1992): Calcite–graphite isotope thermometry: a test for polymetamorphism in marble, Tudor gabbro aureole, Ontario, Canada. *J. Metamorphic Geol.* **10**, 487-501.

FERRY, J.M. & BAUMGARTNER, L. (1987): Thermodynamic models of molecular fluids at the elevated pressures and temperatures of crustal metamorphism. *In* Thermodynamic Modeling of Geological Materials: Minerals, Fluids, and Melts (I.S.E. Carmichael & H.P. Eugster, eds.). *Rev. Mineral.* **17**, 323-365.

GARCÍA DUEÑAS, V. & COMAS, M.C. (1983): Sobre la evolución mesozoica de la plataforma y margen ibéricos correspondientes a las Zonas Externas Béticas. *Actas V Asamb. Nac. Geodesia Geofís.*, 271 (abstr.).

GARCÍA-HERNÁNDEZ, M., LÓPEZ-GARRIDO, A.C., RIVAS, P., SANZ DE GALDEANO, C. & VERA, J.A. (1980): Mesozoic paleogeographic evolution of the External Zones of the Betic Cordillera. *Geol. Mijnb.* **59**(2), 155-168.

HAHN-WEINHEIMER, P. & HIRNER, A. (1981): Isotopic evidence for the origin of graphite. *Geochem. J.* **15**, 9-15.

JAROSEWICH, E., NELEN, J.A. & NORBERG, J.A. (1980): Reference samples for electron microprobe analysis. *Geostandards Newsletters* **4**, 43-47.

JÉBRAK, M. (1992): Les textures intra-filoniennes, marqueurs des conditions hydrauliques et tectoniques. *Chronique de la Recherche Minière* **506**, 25-35.

KRAUTHEIM, G. (1993): *Kristallinitaetsbestimmungen an Schitchtmineralen Illit und Graphit.* Ph.D. thesis, University of Hannover, Hannover, Germany.

KWIECINSKA, B. (1980): Mineralogy of natural graphites. *Polska Akad. Nauk, Prace Mineralogiczne* **67**, 5-79.

LANDIS, C.A. (1971): Graphitization of dispersed carbonaceous material in metamorphic rocks. *Contrib. Mineral. Petrol.* **30**, 34-45.

LUQUE, F.J., BARRENECHEA, J.F. & RODAS, M. (1993): Graphite geothermometry in low and high temperature regimes: two case studies. *Geol. Mag.* **130**, 501-511.

_____, RODAS, M. & GALÁN, E. (1992): Graphite vein mineralization in the ultramafic rocks of southern Spain: mineralogy and genetic relationships. *Mineral. Deposita* **27**, 226-233.

OHMOTO, H. & KERRICK, D.M. (1977): Devolatilization equilibria in graphitic systems. *Am. J. Sci.* **277**, 1013-1044.

PASTERIS, J.D. & CHOU, I-MING (1998): Fluid-deposited graphitic inclusions in quartz: comparison between KTB (German Continental Deep Drilling) core samples and artificially re-equilibrated natural inclusions. *Geochim. Cosmochim. Acta* (in press).

_____, HARRIS, T.N. & SASSANI, D.C. (1995): Interactions of mixed volatile–brine fluids in rocks of the southwestern footwall of the Duluth Complex, Minnesota: evidence from aqueous fluid inclusions. *Am. J. Sci.* **295**, 125-172.

_____ & WOPENKA, B. (1991): Raman spectra of graphite as indicators of degree of metamorphism. *Can. Mineral.* **29**, 1-9.

PEARSON, D.G., BOYD, F.R. & NIXON, P.H. (1990): Graphite-bearing mantle xenoliths from the Kaapvaal Craton: implications for graphite and diamond genesis. *Carnegie Inst. Washington, Yearbook*, 11-19.

PORTUGAL, M., MORATA, D., PUGA, E., DEMANT, A. & AGUIRRE, L. (1995): Evolución geoquímica y temporal del magmatismo básico mesozoico en las zonas externas de las Cordilleras Béticas. *Estudios Geológicos* **51**, 109-118.

PUGA, E. & PORTUGAL, M. (1989): The recrystallization and partial melting of xenoliths of pelitic rocks and their bearing on the contaminated basalts (Subbetic Zone, Spain). *In* Magma-Crust Interactions and Evolution. Theophrastus Publications, S.A., Athens, Greece (115-159).

_____, _____, DÍAZ DE FEDERICO, A., BARGOSSI, G.M. & MORTEN, L. (1989): The evolution of the magmatism in the external zones of the Betic Cordilleras during the Mesozoic. *Geodinamica Acta* **3**(4), 253-266.

RUMBLE, D., III, DUKE, E.F. & HOERING, T.C. (1986): Hydrothermal graphite in New Hampshire: evidence of carbon mobility during regional metamorphism. *Geology* **14**, 452-455.

_____ & HOERING, T.C. (1986): Carbon isotope geochemistry of graphite vein deposits from New Hampshire, U.S.A. *Geochim. Cosmochim. Acta* **50**, 1239-1247.

SCHEELE, N. & HOEFS, J. (1992): Carbon isotope fractionation between calcite, graphite and CO_2: an experimental study. *Contrib. Mineral. Petrol.* **112**, 35-45.

SCHIDLOWSKI, M., HAYES, J.M. & KAPLAN, I.R. (1983): Isotopic inferences of ancient biochemistries: carbon, sulfur, hydrogen, and nitrogen. *In* Earth's Earliest Biosphere: its Origin and Evolution (J.W. Schopf, ed.). Princeton University Press, Princeton, New Jersey (149-186).

SCHREINER, W.N. & JENKINS, R. (1983): Profile fitting for quantitative analysis in X-ray powder diffraction. *Advances in X-Ray Analysis* **26**, 141-147.

STRENS, R.G.J. (1965): The graphite deposit of Seathwaite in Borrowdale, Cumberland. *Geol. Mag.* **102**, 393-406.

WADA, H., TOMITA, T., MATSUURA, K., IUCHI, K., ITO, M. & MORIKIYO, M. (1994): Graphitization of carbonaceous matter during metamorphism with references to carbonate and pelitic rocks of contact and regional metamorphisms, Japan. *Contrib. Mineral. Petrol.* **118**, 217-228.

WALTHER, J. & ALTHAUS, E. (1993): Graphite deposition in tectonically mobilized fault planes of the KTB-pilot drill hole. *In* Kontinentales Tiefbohrprogramm der Bundesrepublik Deutschland (R. Emmermann, J. Lauterjung & T. Umsonst, eds.). *Niedersächsisches Landesamt für Bodenforschung (Hannover, Germany), Rep.* **93-2**, 493-497.

WEIS, P.L., FRIEDMAN, I. & GLEASON, J.P. (1981): The origin of epigenetic graphite: evidence from isotopes. *Geochim. Cosmochim. Acta* **45**, 2325-2332.

WOPENKA, B. & PASTERIS, J.D. (1993): Structural characterization of kerogens to granulite-facies graphite: applicability of Raman microprobe spectroscopy. *Am. Mineral.* **78**, 533-557.

ZIEGENBEIN, D. & JOHANNES, W. (1980): Graphite in C–H–O fluids: an unsuitable compound to buffer fluid composition at temperatures up to 700°C. *Neues Jahrb. Mineral., Monatsh.*, 289-305.

_____ & _____ (1990): Graphit–Fluid-Wechselwirkungen: Einfluß der Graphit-Kristallinität. *In* Kontinentales Tiefbohrprogramm der Bundesrepublik Deutschland (R. Emmermann & P. Giese, eds.). *Niedersächsisches Landesamt für Bodenforschung (Hannover, Germany), Rep.* **90-4**, 559.

_____, SKROTZKI, R., HOEFS, J., MÜLLER, H., REUTEL, C. & EMMERMANN, R. (1989): Fluidtransport und Graphitbildung auf Störungszonen. *In* Kontinentales Tiefbohrprogramm der Bundesrepublik Deutschland (R. Emmermann & P. Giese, eds.). *Niedersächsisches Landesamt für Bodenforschung (Hannover, Germany), Rep.* **89-3**, 46-53.

Received March 7, 1997, revised manuscript accepted June 1, 1997.